Reliability and Failure Analysis of Lead-Free Solder Joints for PBGA Package Under a Cyclic Bending Load

Ilho Kim and Soon-Bok Lee

***Abstract*—Nowadays, interest in the bending reliability of ball grid array packages has increased with the increase in mobile devices. Initially, bending tests were conducted to certify the safety of an electronic package during the manufacturing and shipping processes. But recently, the purpose of the bending test has changed: cyclic bending tests are being used to evaluate the electronic package's endurance against handling damage such as bending, twisting and key pressure. Furthermore, the bending test is being adopted as an alternative to a drop test. In this study, a four-point cyclic bending test was performed under various loading levels to investigate the fatigue behavior of solder joints with chemical compositions of 95.5Sn4.0Ag0.5Cu and 63Sn37Pb. It was found that the lead-free solder has a longer fatigue life than the lead-contained solder when the applied load is low. A finite element analysis (FEA) with plasticity and creep constitutive equations was conducted because there are no suitable sensors to measure stress and strain of solder ball joints directly. From the analysis results, it was found that the inelastic energy dissipation could be used as a good damage parameter. Also, from the inspection of the failure site and the FEA, it was found that the fatigue crack initiated at the exterior solder joints and propagated into the inner solder joints.**

***Index Terms*—Ball grid array (BGA), cyclic bending test, finite element methods (FEM), lead-free solder, Sn-Ag-Cu.**

I. Introduction

RECENTLY, the use of mobile devices has increased: cellular phones, personal data assistants (PDA), MP3 players, DVD players, portable multimedia players (PMP), and so on. In these mobile devices, major failure mechanisms have been recognized as the mechanical load in the electronic packages rather the thermal load which is predominant in the fixed hardware. The recent development trend of electronic packages has changed: the modern requirements for mobile devices have pushed the development of the packages toward smaller, thinner, lighter, and higher density configurations, which weakens the package with regard to mechanical loading. These mechanical loads include the bending, twisting, key pressing, vibration, and shock impact due to dropping.

Various bending tests have been used to quantitatively estimate the reliability of the solder joints [1]–[5]. Three-point cyclic bending tests have been performed by many researchers [1]–[4]. Furthermore, Merchdo *et al.* [4] and Harada *et al.* [5] have used a four-point bending test for the ease of later data analysis since the stress developed at the inner loading span can be assumed to be uniform. Generally, single-side boards with one unit are used for the bending test, but single-side or double-side boards with numerous units are also used [2]–[4]. A board with many units creates a large amount of data obtained in one test; however, it is difficult to maintain a uniform stress in all units. In this study, single-side boards with one unit were tested using the four-point bending loads to analyze the test results easily and accurately. It is difficult to experimentally measure the stress and strain developed at the solder joints during the test, therefore a finite element analysis (FEA) was used. The FEA model includes the creep and plasticity constitutive relations. An analysis on the inelastic strain, energy, and stress was also performed to find an appropriate damage parameter.

II. Experimental Procedure and Results

A. Development of a Cyclic Bending Tester

In this study, an efficient bending test system was developed. A general-purpose hydraulic mechanical system is constructed for a large specimen and thus the resolution of the load-cell was inadequate for small-sized electronic packages. The bending test system used in this study was developed to compensate for the weak points of a hydraulic mechanical system. Figs. 1 and 2 show the schematic diagram and a photograph of the developed system, respectively.

The testing machine applied a load to the specimen via an electro-magnetic coil guided through a linear bushing. Various sensors were attached. A high-resolution load-cell measured the applied loads and these values were used for feedback control. The linear variable displacement transformer (LVDT) for measuring the distance between the two grips was attached at the grips. The failure detection system consisted of a Wheaston-bridge circuit, which includes a daisy chain of specimens as one resistance arm [6]. A strain measurement system using strain gage was also constructed that could measure eight channel strains simultaneously. All of the measured signals were recorded using the data acquisition (DAQ) board of a personal computer (PC). But all of measured data was not recorded. The required memory is too large, so one cycle data

Manuscript received November 16, 2006; revised October 21, 2007. This work was supported by the Ministry of Science and Technology in Korea through "Development of Reliability Design Technique and Life Prediction Model for Electronic Components." This work was recommended for publication by Associate Editor P. Lall upon evaluation of the reviewers comments.

The authors are with the Department of Mechanical Engineering, Korea Advanced Institute of Science and Technology, Daejeon 305-701, Korea (e-mail: seamark@kaist.ac.k; sblee@kaist.ac.kr).

Color versions of one or more of the figures in this paper are available online at http://ieeexplore.ieee.org.

Digital Object Identifier 10.1109/TCAPT.2008.921650

1521-3331/$25.00 © 2008 IEEE

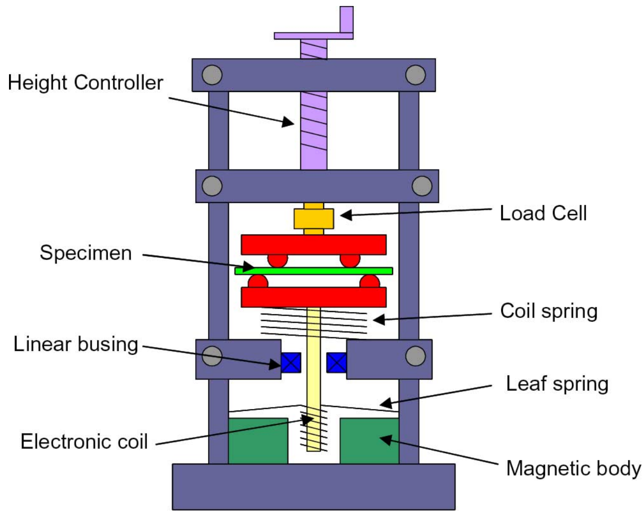

Fig. 1. Schematic drawing of the newly developed bending fatigue testing system.

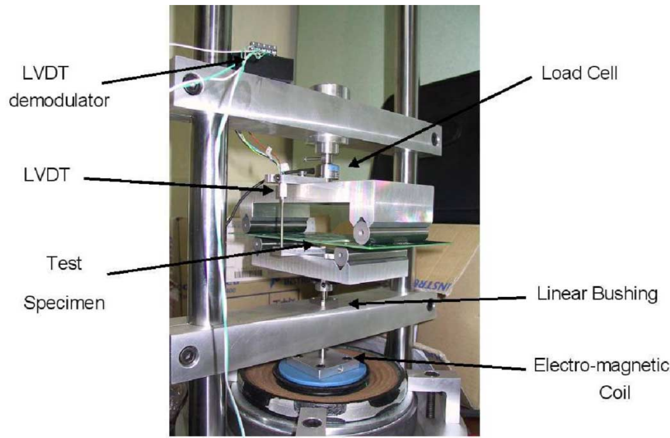

Fig. 2. Real photograph of the newly developed bending fatigue testing system.

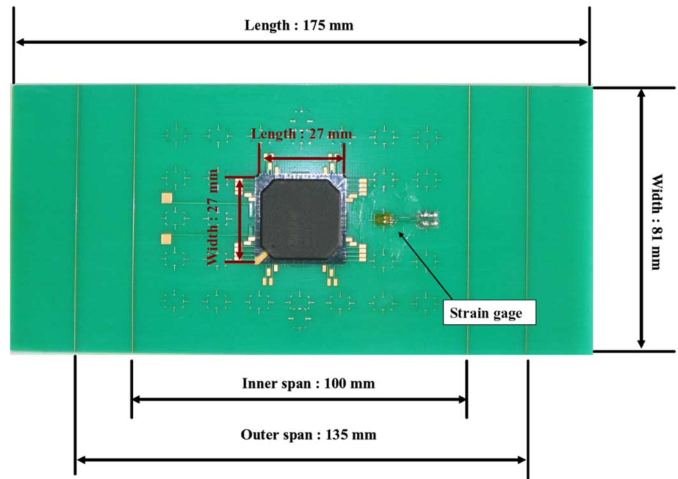

Fig. 3. Specimen for four point bending test, where 256PBGA package is attached to the PWB board.

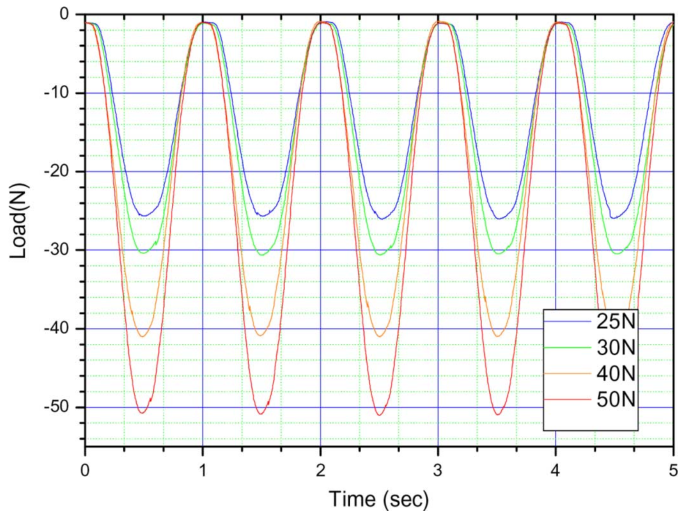

Fig. 4. Applied load profiles.

was recorded at each 10 cycles. In other words, nine cycle's data (9 s) was skipped and then only one cycle's data (1 s) was recorded. The PC also made the actuator-control signal automatically using the proportional-integral-derivative (PID) control algorithm.

B. Test Specimen

The test specimen used in this study was a 256 PBGA (plastic ball grid array) package, which has a $27 \times 27 \times 0.36$ mm substrate with a $10 \times 10 \times 0.3$ mm die and 1.17 mm-thick overmold. Each specimen includes 256 solder balls with a diameter of 760 μm where the ball pitch was 1.27 mm and the solder balls are arranged in 4 peripheral rows. Two types of solder ball materials were used: one is a eutectic lead-contained solder (63Sn37Pb) and the other is a lead-free solder (95.5Sn4.0Ag0.5Cu).

The printed wired board (PWB) size and load span of test specimen were determined through a simple FEA to obtain a uniform stress field near the package. The length, width, inner span, and outer span of PWB were 175, 81, 100, and 135 mm, respectively. The PWB thickness, which has 2 copper layers, was 1.0 mm and the pad diameter was 0.635 mm. Pad is finished by Ni/Au. The marks for the strain gauge to be placed were drawn on the top and bottom surfaces of the PWB. The 256 PBGA and PWB were assembled to make test specimen via a reflow process in a nitrogen environment [7]. Fig. 3 shows the test specimen.

C. Experimental Procedure

In this study, bending fatigue tests were performed using 1 Hz sinusoidal wave with various amplitudes ranging 25 to 60 N; 25, 30, 40, 50 and 60 N. At each loading condition the test was repeated more than five times and the representative value for fatigue life was defined as the average number of cycles. The applied load is shown in Fig. 4. It is noted that the specimen was not fixed on the loading cylinder but was only placed on the cylinder. To maintain the contact between the specimen and the loading cylinder, the minimum applied load is set to 1 N. For example, if the loading amplitude of 30 N is used, the applied load changes from 1 to 31 N.

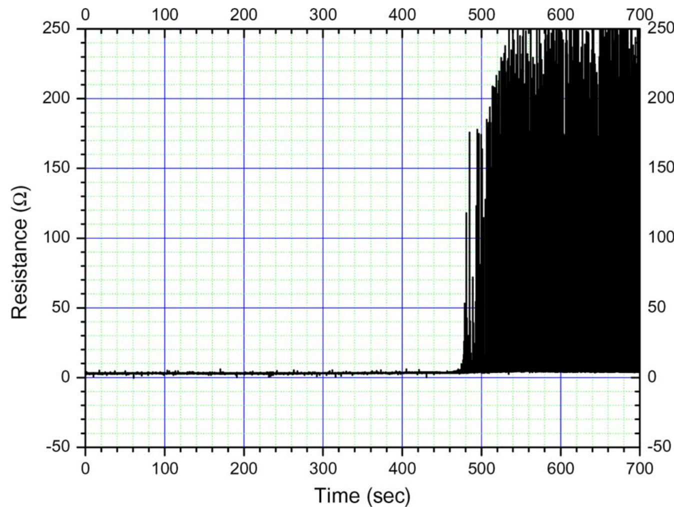

Fig. 5. Variation in the resistance of the daisy chain on the PBGA package with time; an abrupt increase is noted at the onset of failure.

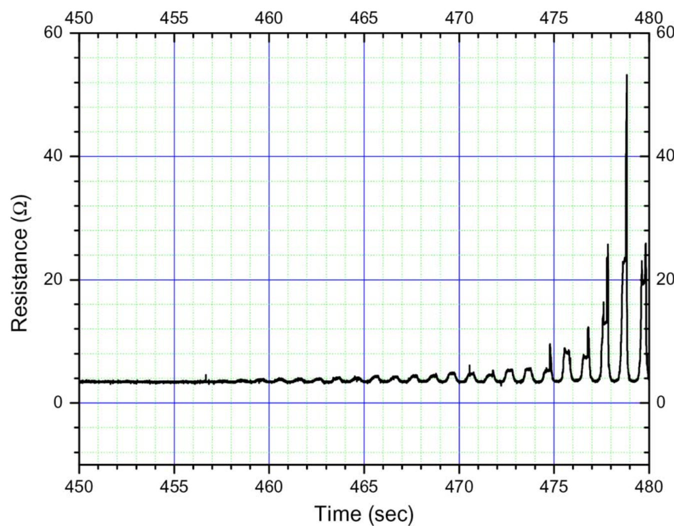

Fig. 6. Magnified view of resistance at failure.

Fatigue failure of a test specimen is defined as the point where the resistance of the daisy chain changes abruptly, as shown in Fig. 5. Because the resistance behavior of a specimen is an irreversible process, once an unstable phenomenon has started it can never become stable again. Hence this failure criterion is thought to be reasonable. Fig. 6 shows a magnified view of the resistance variation when failure occurs.

D. Results

The correlation between the fatigue life cycles and applied loads is presented in Fig. 7. Each data point in Fig. 7 represents the average value of five tests for SnAgCu and six tests for higher load range of SnPb, seven tests for lower load range of SnPb. The results show that the solder having a good fatigue resistance can be reversed depending on the load conditions. The lead-contained solders have a longer fatigue life in the region where the applied load is high. The mechanical fatigue life of lead-free solder is approximately 5600 cycles when the load amplitude is 60 N, but the lead-contained solder has a 1.66 times longer life of approximately 9400 cycles. On the contrary, the lead-free solder sustains more cyclic loads in the low load region. When the applied load amplitude was controlled at 25 N, the fatigue life of the lead-free solder was longer than that of the lead-contained solder; the lead-contained and lead-free solders sustained 220 000 and 240 000 cycles, respectively.

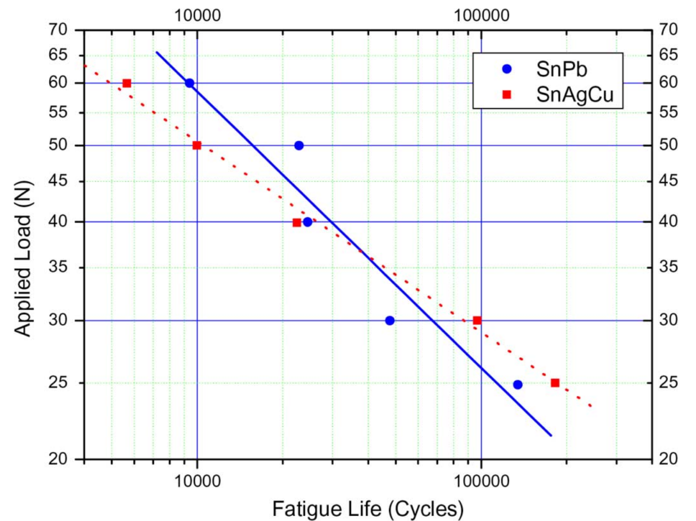

Fig. 7. Applied load versus bending fatigue life curve of lead-contained and lead-free solders.

A similar trend was detected between the cyclic bending test and the thermal cycling test. When the applied thermal stress was high, the lead-contained solder had a longer fatigue life than the lead-free solder. On the contrary, when the applied thermal stress was low, the lead-free solder had a longer fatigue life [8]–[10]. The better performance solder on a certain load is changeable, because two solder has totally different chemical composition. This phenomenon is not uncommon in metals. For example S55C steel has 10 000 and 1 000 000 fatigue life at about 330 MPa and about 250 MPa, respectively, but the 1.6C-1.95Si steel has the same fatigue life at about 450 MPa and about 240 MPa, respectively [11]. S55C steel has a good fatigue resistance at the low load region, but 1.6C–1.95 Si steel has long fatigue life at the high load region. This means that the better performance steel can be reversed depending on the load level as the solders did in this research.

III. Failure Analysis

To identify the cracking behavior in the solder joints, the failed specimen was sectioned. As shown in Fig. 8, both sides of the package, where the stress developed is maximized, were selected as inspection locations. The reason for the maximum stress to take place at both sides of the package is the effective elastic modulus changed at those positions.

Fig. 9 shows a section view of the 17th to 20th solder joints where each solder position is indicated in Fig. 8. As shown in Fig. 9, the fatigue crack length increases as the distance from the center increases. The crack length of 17th solder joint is half the solder diameter, but the crack in the 18th to 20th solders has propagated through the entire length. Furthermore, the gap of the two parts separated by the crack is maximized at the outermost solder joint, because the plastic deformation of the

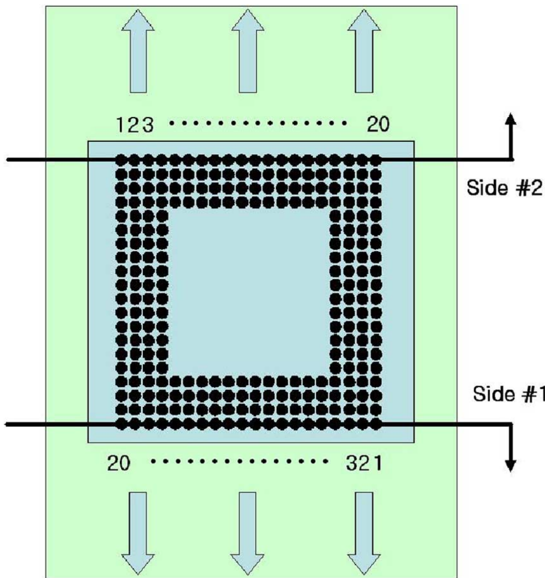

Fig. 8. Sectioning locations for the crack observation in the specimen.

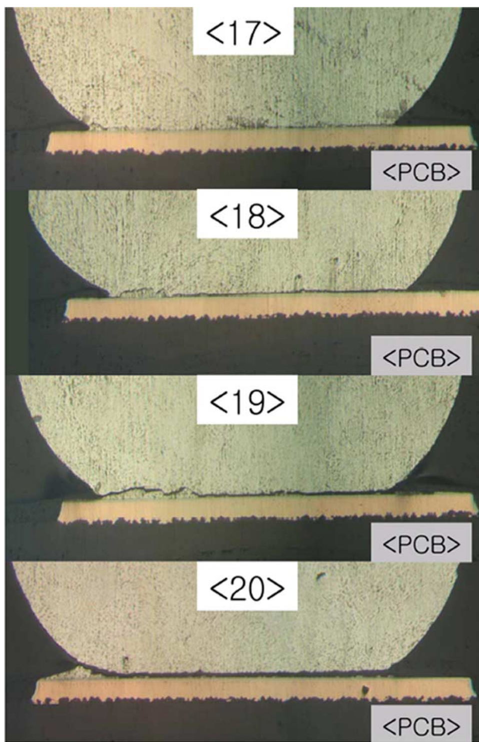

Fig. 9. Optical micrographs showing the cracks at each solder joint in the SnPb-PBGA package.

inner solder joint causes the outside solder to lift after the outer solder failed. As shown in Fig. 9, the crack is initiated at the outermost solder joints and propagated through to the inner solder joints. The cracks were observed only at the interface between the solder and the pad on PWB.

Fig. 10 shows a section view of another specimen in which the fatigue crack was observed only at each outermost solder joint. Based on these results it is believed that the fatigue crack was initiated at each outermost solder joint concurrently. These

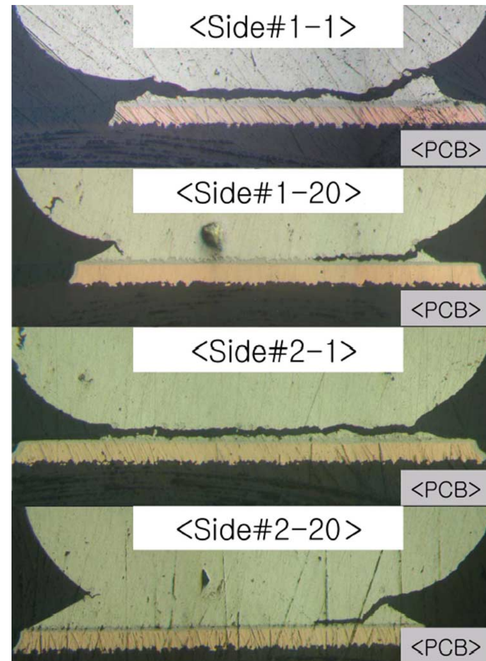

Fig. 10. Optical micrographs depicting the exterior solder joints at each corner in SnAgCu-PBGA package.

results agree well with the FE analysis results, described in the following section.

IV. Finite Element Analysis

A. Modeling

A 3-D FEA model was constructed using the modeling software PATRAN. A FEA using ABAQUS was performed to extract the stress and strain induced in the solder joints. Due to the symmetry of the specimen geometry, only a quarter of bending cycling specimen was modeled. To achieve calculation efficiency, the high stress solder joints were meshed finely and the remainder was meshed coarsely. The FE analysis model for the cyclic bending test consisted of 60 656 elements and 75 343 nodes; this model is depicted in Fig. 11. The material properties used in the model were taken from Park [12], Hong [13], and Lau *et al.* [14] where 95.5Sn3.9Ag0.6Cu was selected for the 95.5Sn4.0Ag0.5Cu solder due to the lack of available material data. A constitutive model which includes both creep and plasticity was also employed (see Table I). The loading bar was modeled as an analytical rigid body and located in the same position as that of the experiment performed.

B. Analysis Results

Fig. 12 shows the distribution of the von Mises stress in the solder joints as a load of 50 N is applied. The solder joints closely located to the loading bar sustains larger stress than the other joints. Also the developed stress decrease as the distance from the loading bar increase. Another stress concentration occurred along to the PWB width direction (see Fig. 11) due to the Poisson's ratio, where the stress is maximized at the outmost solder. The stress component in the PWB width direction is smaller than that in PWB length direction. The stress at the

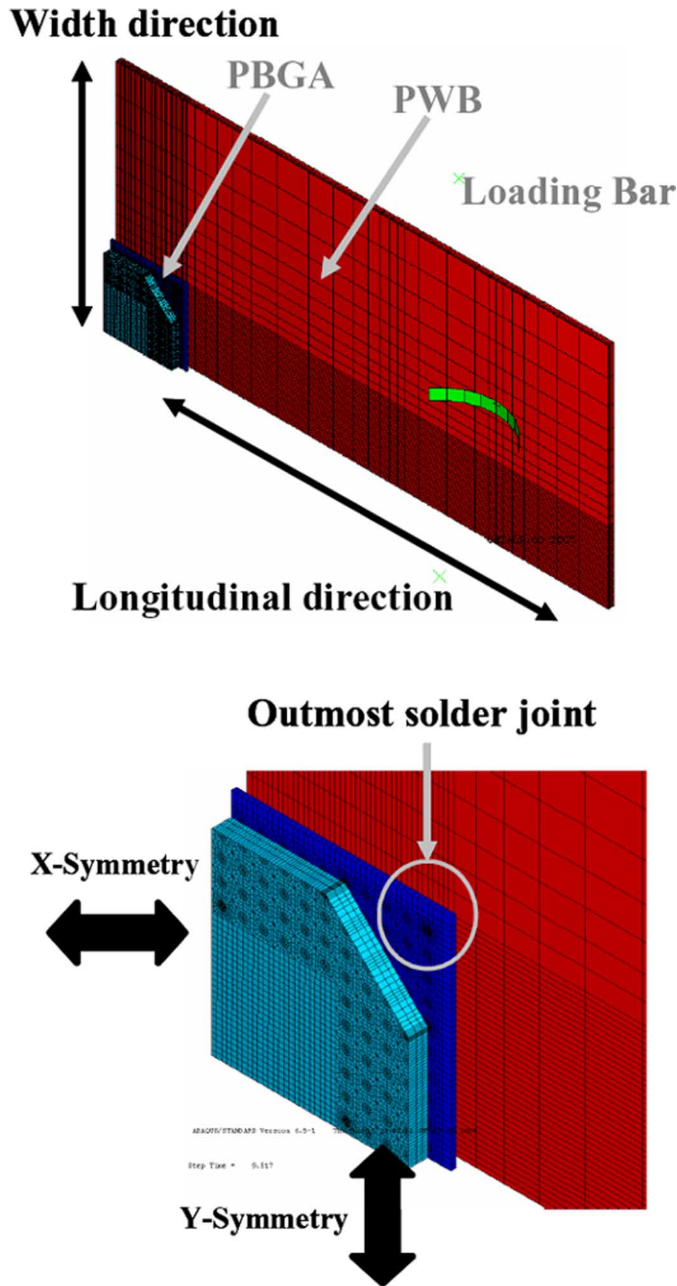

Fig. 11. Visco-plastic finite element model for the bending fatigue test.

TABLE I
MECHANICAL PROPERTIES OF TESTING MATERIALS

Material	Elastic Modulus (MPa)	Poisson Ratio	Yield Strength (MPa)	Tangent Modulus (MPa)
Sn37Pb	43251	0.3628	29.1	-
Sn4.0Ag0.5Cu	53000	0.4	30	1500
Copper	117000	0.34	69.0	-
FR-4	22000(x,y)	0.28	elastic	elastic
	10000(z)	0.11	elastic	elastic
Silicon	130008	0.2782	elastic	elastic
Epoxy	25845	0.35	elastic	elastic
Creep behavior	$\dot{\varepsilon} = A[\sinh(B\sigma)]^n \exp\left(-\frac{Q}{RT}\right)$			
	$A(s^{-1})$	$B(MPa^{-1})$	n	Q(J/mole)
Sn37Pb	12423	0.126	1.89	61417
Sn4.0Ag0.5Cu	44100	0.005	4.2	44995

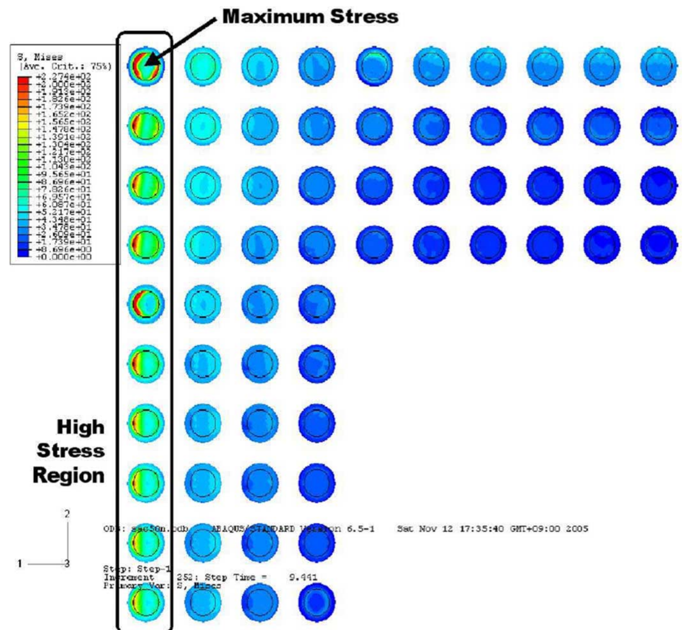

Fig. 12. Von Mises stress distribution at the solder joints.

outermost solder joint is the result of combination of stress components in PWB length direction and PWB width direction; thus the outermost solder joint failed first. These results are in good agreement with the physical inspection of the failed specimen.

Plastic deformation is more predominant because the testing frequency is fast (1 Hz) and the applied load is relatively high. The inelastic energy dissipated by the creep deformation is a twentieth smaller than that by the plastic deformation. Figs. 13 and 14 show the plastic energy density of critical point in the lead-free and lead-contained solders, respectively. In those figures the plastic energy density increases with the number of cycles.

The correlation between the total inelastic energy density and the fatigue life is depicted in Fig. 15, where the total inelastic energy density is the sum of the plastic and creep energy densities at the stable state (after five cycles) and can be calculated using (1) where $\Delta W_{\text{total}}, V_i, dW_i$ represent the total inelastic energy density, volume and inelastic energy density increment of i-th element, respectively. Volume averaging was conducted on the first layer elements at the failure site

$$\Delta W_{\text{total}} = \frac{\sum_{i=1}^{n} dW_i V_i}{\sum_{i=1}^{n} V_i}. \quad (1)$$

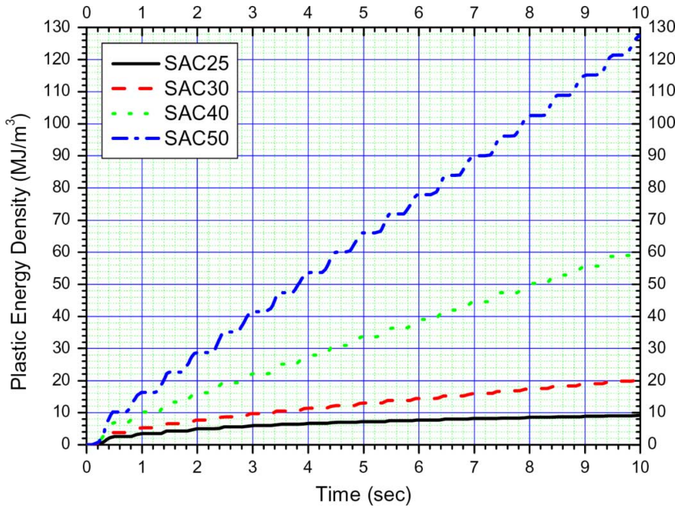

Fig. 13. Plastic energy density at the critical point in the lead-free solder.

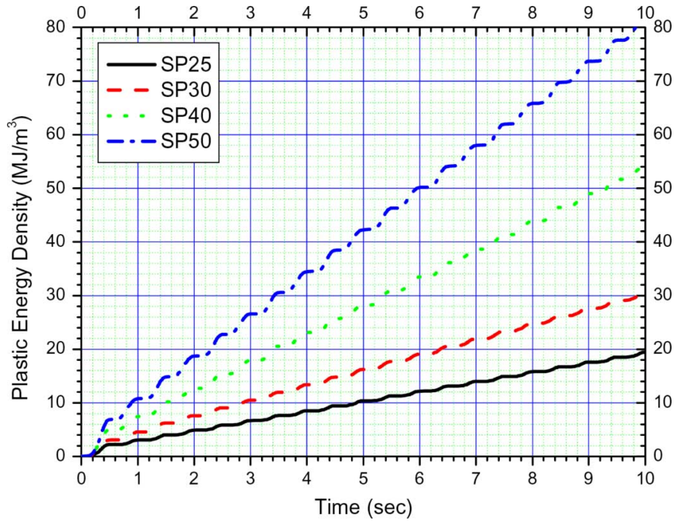

Fig. 14. Plastic energy density at the critical point in the lead-contained solder.

The results revealed that the lead-contained solders have higher fatigue resistances than the lead-free solders, in some sense. However, it should be noted that a direct comparison between fatigue lives of the solder materials will not provide any meaningful insight. First, these two solders have different material ductility coefficients and fatigue exponents in the Morrow energy model; so two curves have different slopes and y-axis intercepts. Morrow's life prediction model was shown in (2), where m is fatigue exponent, C is material ductility coefficient and ΔW is total inelastic energy density (J/m ^{3}), respectively

$$N_f^m \Delta W = C. \tag{2}$$

Second, despite an identical applied load, the stress and strain induced in the lead-free solder are different from those of the lead-contained solder; because the elastic modulus, yield stress, and tangent modulus of the lead-free solder are different from those of the lead-contained solder. Accordingly the inelastic dissipation energies calculated from the stress and strain are also distinct from each other and this can be confirmed in Fig. 15. The lead-contained solder has more inelastic energy dissipation

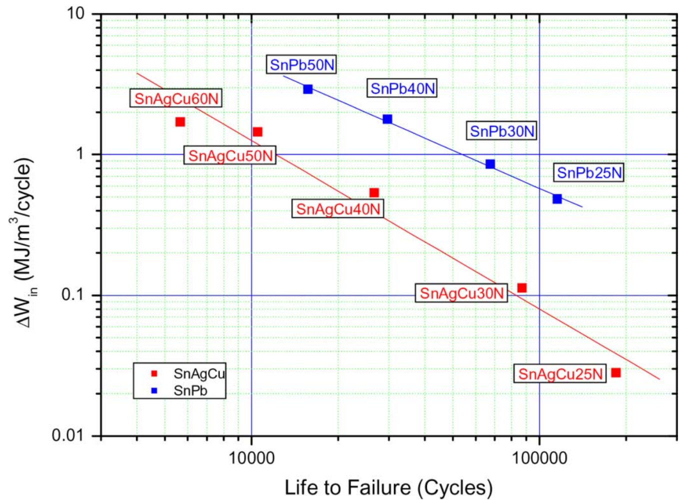

Fig. 15. Inelastic energy dissipation per cycle (ΔW_{in}) versus fatigue life curves.

per cycle at the same loading condition, because it has lower yield stress than the lead-free solder. As shown in Fig. 15, in the lead-contained solder, the inelastic energy dissipation per cycle changes from 4.84×10^{-1} to 2.91 MJ/m^3/cycle as the applied loads increases from 25 to 50 N. However, in the lead-free solder, it shows a different behavior; the inelastic energy dissipation changes from 2.81×10^{-2} to 1.45 MJ/m^3/cycle in the same applied load range. In the log-log scale, as shown in Fig. 15, the inelastic energy dissipation per cycle and fatigue life has a linear relation. This indicates that the inelastic energy dissipation per cycle is a suitable damage parameter in the cyclic bending test to predict fatigue life. The life prediction models based on Morrow model are proposed as (3) and (4).

For 95.5Sn4.0Ag0.5Cu

$$N_f = 12152 \Delta W_{\mathrm{in}}^{-0.83499}. \tag{3}$$

For 63Sn37Pb

$$N_f = 54094 \Delta W_{\mathrm{in}}^{-1.11454}. \tag{4}$$

V. Conclusion

A mechanical cyclic bending testing system was developed to investigate the fatigue behavior of the solder joints for PBGA packages, and a non-linear finite element model considering creep and plastic constitutive models was used to analyze the stress and strain distribution induced during the test. It was found that the lead-free solder (95.5Sn4.0Ag0.5Cu) has a stronger fatigue resistance than the lead-contained solder (63Sn37Pb) under low loading levels. When the applied load increased, however, the lead-contained solder has a longer fatigue life. The maximum stress and inelastic deformation were developed in the outermost solder joints on the PWB side, and thus the crack initiated from those positions and propagated into the inward direction. This fact could also be confirmed through the failure analysis using the section inspection. From the inelastic energy dissipation per cycle versus fatigue life curve, it was found that the inelastic energy dissipation is a good damage parameter to predict the fatigue lives of the solder joints.

ACKNOWLEDGMENT

The authors would like to thank Dr. S.-G. Hong for his support and encouragement.

REFERENCES

[1] J. D. Wu, S. H. Ho, P. J. Zheng, C. C. Liao, and S. C. Hung, "An experimental study of failure and fatigue life of a stacked CSP subjected to cyclic bending," in *Proc. 2001 Electron. Comp. Technol. Conf.*, Orlando, FL, May 29–Jun. 1 2001, pp. 1081–1086.

[2] D. T. Rooney, N. T. Castello, M. Cibulsky, D. Abbott, and D. Xie, "Materials characterization of the effect of mechanical bending on area array package interconnects," *Microelectron. Reliab.*, vol. 44, pp. 275–285, 2004.

[3] S. Shetty and T. Reinikainen, "Three- and four-point bend testing for electronic packages," *J. Electron. Packag.*, vol. 125, no. 4, pp. 556–561, 2003.

[4] L. L. Mercado, B. Phillips, S. Sahasrabudhe, J. P. Sedillo, D. Bray, and E. Monroe, "Use-condition-based cyclic bend test development for handheld components," in *Proc. Electron. Comp. Technol. Conf.*, Las Vegas, NV, Jun. 1–4, 2004, pp. 1279–1287.

[5] K. Harada, S. Baba, Q. Wu, H. Matsushima, T. Matsunaga, and Y. Uegai, "Analysis of solder joint fracture under mechanical bending test," in *Proc. Electron. Comp. Technol. Conf.*, New Orleans, LA, May 27–30, 2003, pp. 1731–1737.

[6] I. Kim and S.-B. Lee, "Reliability assessment of BGA solder joints under cyclic bending loads," in *Proc. Electron. Mater. Packag. (EMAP'05)*, Tokyo, Japan, Dec. 11–14, 2005, pp. 27–32.

[7] I. Kim *et al.*, "Development of reliability design technique and life prediction model for electronic components (first stage report)," CARE Lab, KAIST, 2005.

[8] I. Kim, T.-S. Park, and S.-B. Lee, "A comparative study of the fatigue behavior of SnAgCu and SbPb solder joints.," *Trans. Korean Soc. Mech. Eng. (A)*, vol. 28, no. 12, pp. 1856–1863, 2004.

[9] I. Kim, T.-S. Park, S. Y. Yang, and S.-B. Lee, "A comparative study of the fatigue behavior of SnAgCu and SnPb solder joints," *Key Eng. Mater.*, vol. 297–300, pp. 831–836, 2005.

[10] A. Schubert, R. Dudek, E. Auerswald, A. Gollhardt, B. Michel, and H. Reichl, "Fatigue life models for SnAgCu and SnPb solder joints evaluated by experiments and simulation," in *Proc. Electron. Comp. Technol. Conf.*, New Orleans, LA, May 27–30, 2003, pp. 603–610.

[11] "The Society of Materials Science," in *Databook on Fatigue Strength of Metallic Materials*. Tokyo, Japan: Elsevier Science B.V., 1996, pp. 245–318.

[12] T.-S. Park, "A Study on Mechanical Fatigue Behaviors of Ball Grid Array Solder Joints for Electronic Packaging," Ph.D. dissertation, Daejeon, Korea, 2004.

[13] B. Z. Hong, "Thermal fatigue analysis of a CBGA package with lead-free solder fillets," in *Proc. InterSoc. Conf. Thermal Phenom.*, Seattle, WA, May 27–30, 1998, pp. 205–211.

[14] J. Lau, W. Dauksher, and P. Vianco, "Acceleration models, constitutive equations, and reliability of lead-free solders and joints," in *Proc. Electron. Comp. Technol. Conf.*, New Orleans, LA, May 27–30, 2003, pp. 229–236.

Ilho Kim received the M.S. degree in mechanical engineering from the Korean Advanced Institute of Science and Technology, Daejeon, Korea, in 2004 where he is currently pursuing the Ph.D. degree.

His research is the reliability physics of solder materials and he has a special focus on fatigue behavior and finite element analysis.

Soon-Bok Lee received the B.Sc. degree in mechanical engineering from Seoul National University, Seoul, Korea, in 1974, the M.S. degree from the Korea Advanced Institute of Science and Technology (KAIST), Daejeon, in 1976, and the Ph.D. degree in mechanical engineering from Stanford University, Stanford, CA, in 1980.

After joining KAIST in 1988, he has subsequently become a Professor with the Department of Mechanical Engineering. His technical interests include reliability in electronics packaging, fatigue and fracture mechanics, and structural integrity including MEMS and thin film. He is actively involved in the National Reliability Enhancement Program as a Committee Member of the National Reliability Counsel for Parts and Materials, Ministry of Commerce, Industry and Energy (MOCIE).

Dr. Lee has organized the Third International Symposium on Electronics Materials and Packaging 2001 (EMAP'01) and Fifth International Conference on Experimental Mechanics (ICEM'06) as a General Chairman.